April 24, 2020

Platte River Fall 2019, Nebraska

Topobathymetric Lidar Technical Data Report

Prepared For:

Headwaters Corporation

Justin Brei
Headwaters Corporation
4111 4th Avenue, Suite 6
Kearney, NE 68845
PH: 308-237-5728, ext. 4

Prepared By:

QSI Corvallis
1100 NE Circle Blvd, Ste. 126
Corvallis, OR 97330
PH: 541-752-1204

TABLE OF CONTENTS

Cover Photo: A view of the Platte River topobathymetric digital elevation model colored by elevation, and overlaid with the above-ground lidar returns colored using RGB imagery.

INTRODUCTION

A scenic photo from the Platte River project site, taken in November 2019.

In May 2016, Quantum Spatial (QSI) was contracted by Headwaters Corporation to collect topobathymetric lidar data and digital imagery in the fall of 2019 as part of a multi-year (2016 – 2019) contract over the Platte River in Nebraska. This data collection represents the final data collection in QSI's ongoing partnership with Headwaters Corporation to provide data aiding in the Platte River Recovery Implementation Program. The program is aimed at enhancing, restoring, and protecting the habitat for the Whooping Crane, Least Tern, Piping Plover, and Pallid Sturgeon species within the project area.

This report accompanies the final delivered topobathymetric lidar data and documents contract specifications, data acquisition procedures, processing methods, and accuracy assessment of the final dataset. Acquisition dates and acreage are shown in Table 1, a complete list of contracted deliverables provided to Headwaters Corporation is shown in Table 2, and the project extent is shown in Figure 1.

Table 1: Acquisition dates, acreage, and data types collected on the Platte River Fall 2019 site

Project Site	Total Acres	Acquisition Dates	Data Type
Platte River Fall 2019, Nebraska	92,808	11/16/2019 – 11/20/2019, 11/22/2019, 11/23/2019	Topobathymetric Lidar

Deliverable Products

Table 2: Products delivered to Headwaters Corporation for the Platte River Fall 2019 site

Platte River Fall 2019 Lidar Products Projection: Nebraska State Plane Horizontal Datum: NAD83 (2011) Vertical Datum: NAVD88 (GEOID03) Units: US Survey Feet	
Topobathymetric LiDAR	
Points	LAS v 1.4 • All Classified Returns
Rasters	3.0 Foot ERDAS Imagine files (*.img) • Unclipped Topobathymetric Bare Earth Digital Elevation Model (DEM) • Clipped Topobathymetric Bare Earth Digital Elevation Model (DEM) • Bare Earth and Water Surface Digital Elevation Model (DEM), with Hydroflattened Ponds • Highest Hit Digital Surface Model (DSM) • Topobathymetric Depth Model 1.5 Foot GeoTiffs • Green Sensor Intensity Images • NIR Sensor Intensity Images
Vectors	Shapefiles (*.shp) • Project Boundary • Lidar Tile Index (1,500 ft x 1,500 ft) • Raster Index • Bathymetric Coverage Polygon • Hydroflattened Pond Breaklines with Z values • Water's Edge Breaklines without Z values (used for bathymetric refraction correction and lidar point classification) • Ground Survey Shapes

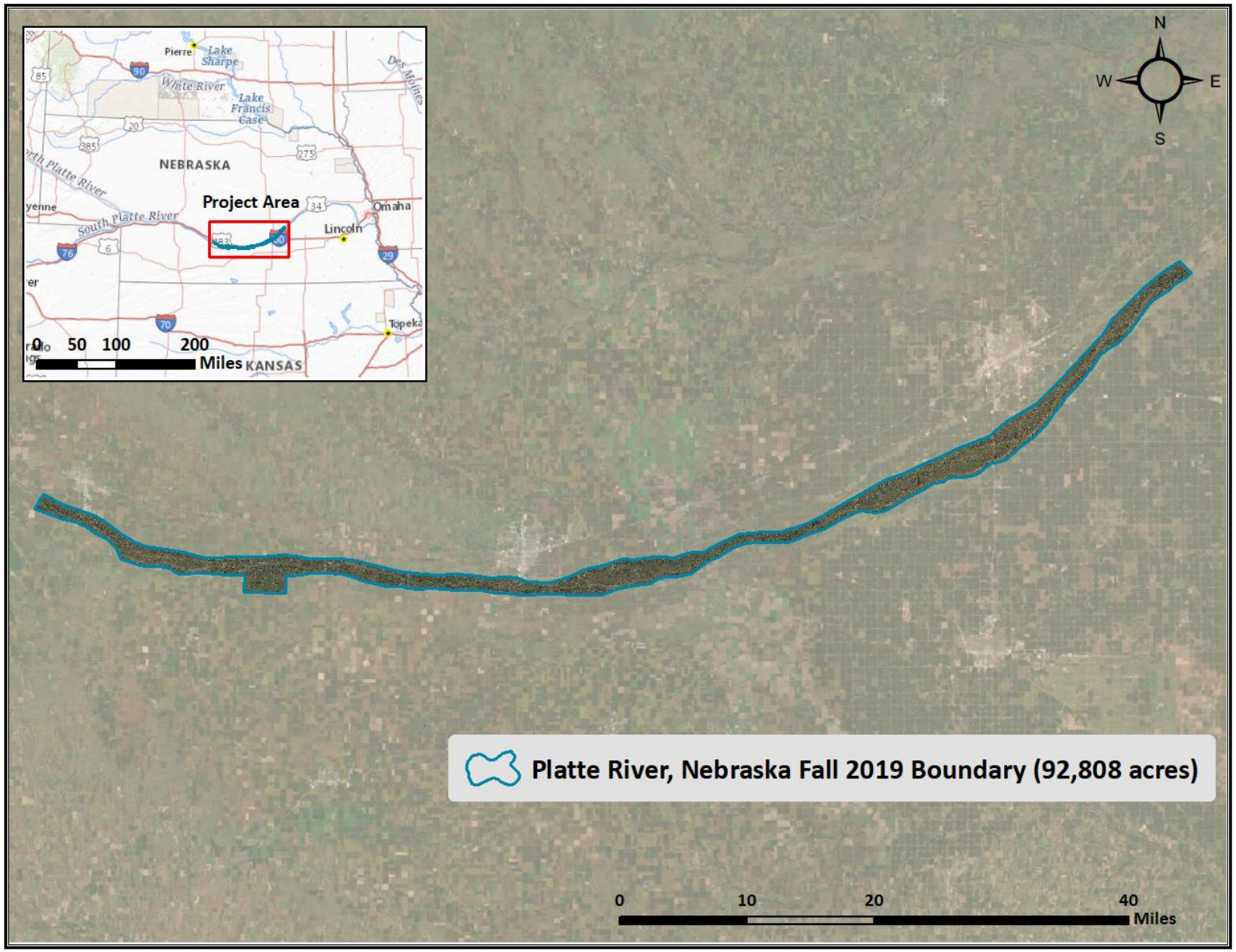

Figure 1: Location map of the Platte River Fall 2019 site in Nebraska

ACQUISITION

QSI's Cessna Caravan

Planning

In preparation for data collection, QSI reviewed the project area and developed a specialized flight plan to ensure complete coverage of the Platte River Fall 2019 Lidar study area at the target combined point density of ≥6 points/m^2. Acquisition parameters including orientation relative to terrain, flight altitude, pulse rate, scan angle, and ground speed were adapted to optimize flight paths and flight times while meeting all contract specifications.

Factors such as satellite constellation availability and weather windows must be considered during the planning stage. Any weather hazards or conditions affecting the flight were continuously monitored due to their potential impact on the daily success of airborne and ground operations. Turbidity readings were monitored throughout acquisition and resulted in average values between 9.46 and 20.9 NTU. In addition, logistical considerations including private property access, potential air space restrictions, and channel flow rates and gage heights were reviewed (Figure 2 and Figure 3).

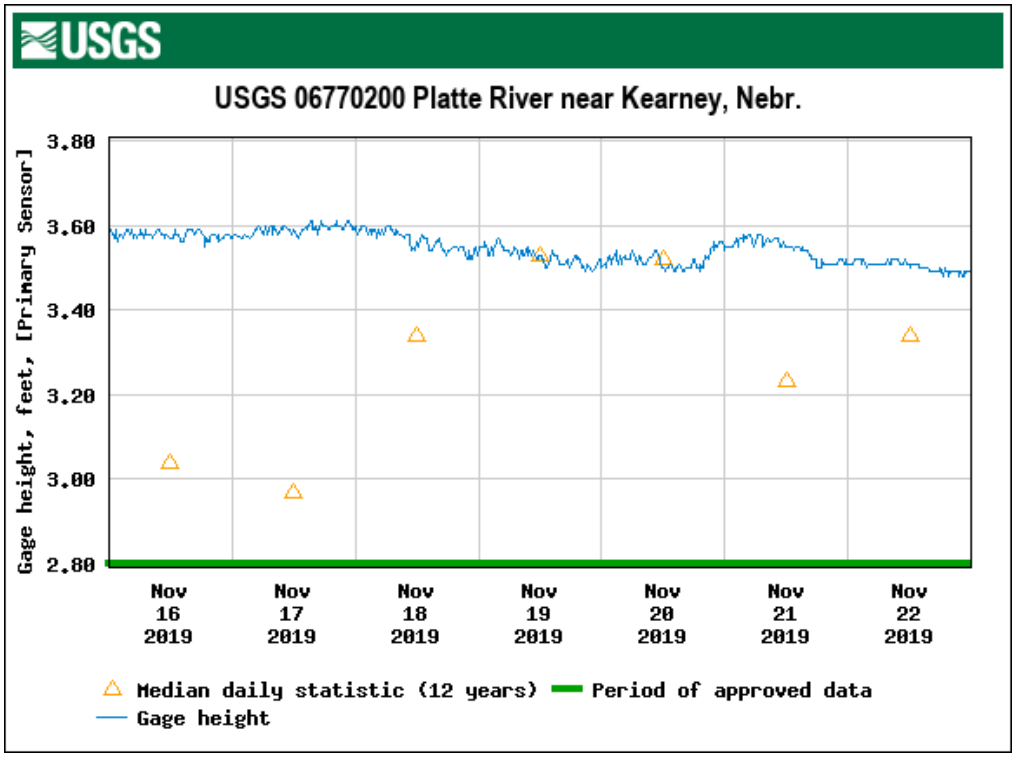

Figure 2: USGS Station 06770200 gage height along the Platte River at the time of LiDAR acquisition.

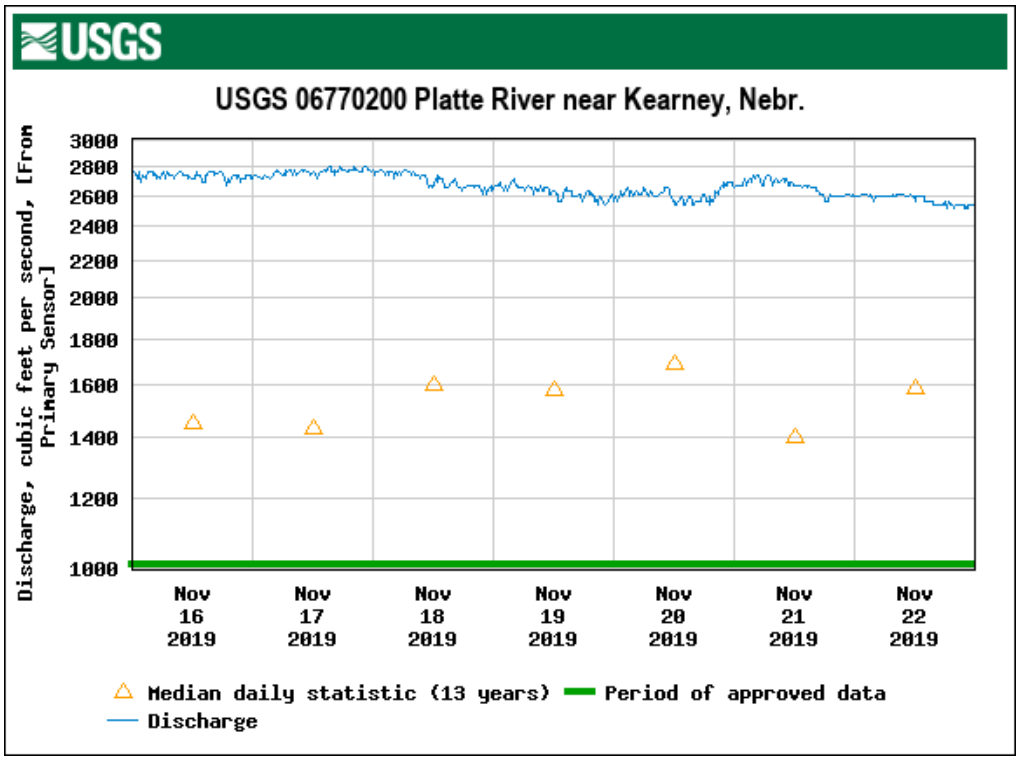

Figure 3: USGS Station 06770200 flow rates along the Platte River at the time of LiDAR acquisition.

Water clarity photos taken by QSI's Ground Professional, along the Platte River on November 16th and 20th, 2019.

Airborne Lidar Survey

The lidar survey was accomplished using a Riegl VQ-880-GII green laser system mounted in a Cessna Caravan. The Riegl VQ-880-GII's integrated NIR laser (λ=1064 nm) adds additional topography data and aids in water surface modeling. The recorded waveform enables range measurements for all discernible targets for a given pulse. The typical number of returns digitized from a single pulse range from 1 to 15 for the Platte River Fall 2019 project area. It is not uncommon for some types of surfaces (e.g., dense vegetation or water) to return fewer pulses to the lidar sensor than the laser originally emitted. The discrepancy between first return and overall delivered density will vary depending on terrain, land cover, and the prevalence of water bodies. Table 3 summarizes the settings used to yield an average pulse density of ≥6 pulses/m^2 over the Platte River Fall 2019 project area.

Table 3: LiDAR specifications and survey settings

LiDAR Survey Settings & Specifications		
Acquisition Dates	11/16/19 – 11/23/19	11/16/19 – 11/23/19
Aircraft Used	Cessna Caravan	Cessna Caravan
Sensor	Riegl	Riegl
Laser	VQ-880GII	VQ-880GII-IR
Maximum Returns	15	15
Resolution/Density	Average 6 pulses/m^2	Average 6 pulses/m^2
Nominal Pulse Spacing	0.41 m	0.41 m
Survey Altitude (AGL)	450 m	450 m
Survey speed	110 knots	110 knots
Field of View	40°	40°
Mirror Scan Rate	80 lines/second	Uniform Point Spacing
Target Pulse Rate	200 kHz	300 kHz
Pulse Length	1.5 ns	3 ns
Laser Pulse Footprint Diameter	31.5 cm	9 cm
Central Wavelength	532 nm	1064 nm
Pulse Mode	Multiple Times Around (MTA)	Multiple Times Around (MTA)
Beam Divergence	0.7 mrad	0.2 mrad
Swath Width	327.57 m	327.57 m
Swath Overlap	55%	55%
Intensity	16-bit	16-bit
Accuracy	$RMSE_Z \leq 15$ cm	$RMSE_Z \leq 15$ cm

All areas were surveyed with an opposing flight line side-lap of ≥55% (≥110% overlap) in order to reduce laser shadowing and increase surface laser painting. To accurately solve for laser point position (geographic coordinates x, y and z), the positional coordinates of the airborne sensor and the attitude of the aircraft were recorded continuously throughout the lidar data collection mission. Position of the aircraft was measured twice per second (2 Hz) by an onboard differential GPS unit, and aircraft attitude was measured 200 times per second (200 Hz) as pitch, roll and yaw (heading) from an onboard inertial measurement unit (IMU). To allow for post-processing correction and calibration, aircraft and sensor position and attitude data are indexed by GPS time.

Ground Survey

Ground control surveys, including base stations and ground survey points (GSPs), were conducted to support the airborne acquisition. Ground control data were used to geospatially correct the aircraft positional coordinate data and to perform quality assurance checks on final lidar data.

Base Stations

Continuously Operating Reference Stations (CORS) were used as base stations for collection of ground survey points using real time kinematic (RTK) survey techniques. Base station locations were selected with consideration for satellite visibility, field crew safety, and optimal location for GSP coverage. QSI utilized two existing HxGN SmartNET reference stations, and two existing Trimble VRSNow reference stations for the Platte River Fall 2019 Lidar project (Table 4, Figure 4).

Table 4: Nebraska CORS positions for the Platte River Fall 2019 acquisition. Coordinates are on the NAD83 (2011) datum, epoch 2010.00

CORS ID	Latitude	Longitude	Ellipsoid (meters)	Network
NEDO	40° 46' 39.11703"	-98° 22' 36.49354"	576.962	VRSNow
NEGN	40° 54' 37.07491"	-98° 22' 51.42422"	555.418	SmartNET
NEKY	40° 42' 38.93410"	-99° 04' 44.99790"	647.063	SmartNET
NELN	40° 46' 05.66516"	-99° 42' 43.38894"	708.806	VRSNow

To correct the continuously recorded onboard measurements of the aircraft position, QSI utilized static Global Navigation Satellite System (GNSS) data collected at 1 Hz recording frequency by the base station. During post-processing, the static GPS data were triangulated with nearby Continuously Operating Reference Stations (CORS) using the Online Positioning User Service (OPUS) to verify and update record positions as needed to align with the National Spatial Reference System (NSRS).

Ground Survey Points (GSPs)

Ground survey points were collected using real time kinematic (RTK) survey techniques. For RTK surveys, a roving receiver receives corrections from a nearby base station or Real-Time Network (RTN) via radio or cellular network, enabling rapid collection of points with relative errors less than 1.5 cm horizontal and 2.0 cm vertical. RTK surveys record data while stationary for at least five seconds, calculating the position using at least three one-second epochs. All GSP measurements were made during periods with a Position Dilution of Precision (PDOP) of ≤ 3.0 with at least six satellites in view of the stationary and roving receivers. See Table 5 for QSI ground survey equipment information.

GSPs were collected in areas where good satellite visibility was achieved on paved roads and other hard surfaces such as gravel or packed dirt roads. GSP measurements were not taken on highly reflective surfaces such as center line stripes or lane markings on roads due to the increased noise seen in the laser returns over these surfaces. GSPs were collected within as many flightlines as possible; however, the distribution of GSPs depended on ground access constraints and monument locations and may not be equitably distributed throughout the study area (Figure 4).

Table 5: QSI ground survey equipment identification

Receiver Model	Antenna	OPUS Antenna ID	Use
Trimble R8	Integrated Antenna	TRM_R8_GNSS	Rover

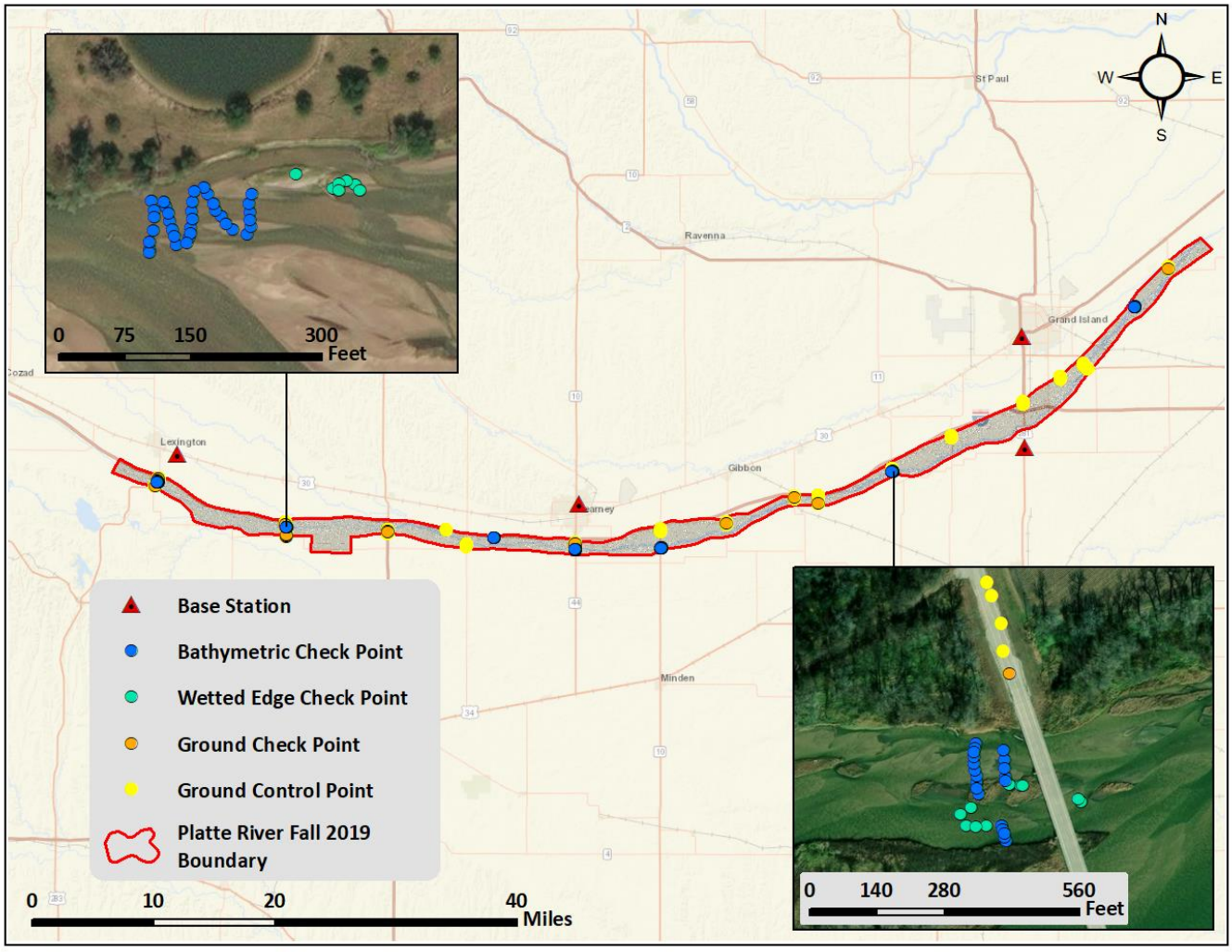

Figure 4: Ground survey location map

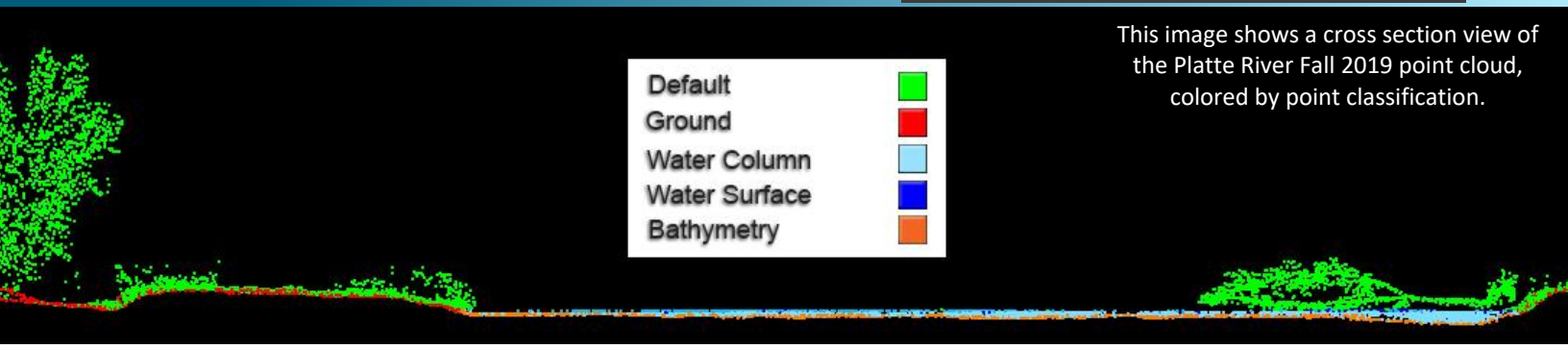

This image shows a cross section view of the Platte River Fall 2019 point cloud, colored by point classification.

Upon completion of data acquisition, QSI processing staff initiated a suite of automated and manual techniques to process the data into the requested deliverables. Processing tasks included GPS control computations, smoothed best estimate trajectory (SBET) calculations, kinematic corrections, calculation of laser point position, sensor and data calibration for optimal relative and absolute accuracy, and lidar point classification (Table 6).

Riegl's RiProcess software was used to facilitate bathymetric return processing. Once bathymetric were differentiated, they were spatially corrected for refraction through the water column based on angle of incidence of the laser. QSI refracted water column points using QSI's proprietary LAS software, LAS Monkey. The resulting point cloud data were classified using both manual and techniques. Processing methodologies were tailored for the landscape. Brief descriptions of these are shown in (

Table 7).

Table 6: ASPRS LAS classification standards applied to the Platte River Fall 2019 dataset

Classification Number	Classification Name	Classification Description
1	Default/Unclassified	Laser returns that are not included in the ground class, composed of vegetation and anthropogenic features
1-O	Overlap/Edge Clip	Flightline edge overlap clipped to maintain contracted scan angles
2	Ground	Laser returns that are determined to be ground using automated and manual cleaning algorithms
7	Noise	Laser returns that are often associated with birds, scattering from reflective surfaces, or artificial points below the ground surface
9	Water	NIR Laser returns that are determined to be water using automated and manual cleaning algorithms
40	Bathymetric Bottom	Refracted Riegl sensor returns that fall within the water's edge breakline which characterize the submerged topography.
41	Water Surface	Green laser returns that are determined to be water surface points using automated and manual cleaning algorithms.
45	Water Column	Refracted Riegl sensor returns that are determined to be water using automated and manual cleaning algorithms.

Table 7: Lidar processing workflow

LiDAR Processing Step	Software Used
Resolve kinematic corrections for aircraft position data using kinematic aircraft GPS and static ground GPS data. Develop a smoothed best estimate of trajectory (SBET) file that blends post-processed aircraft position with sensor head position and attitude recorded throughout the survey.	POSPac MMS v.8.2
Calculate laser point position by associating SBET position to each laser point return time, scan angle, intensity, etc. Create raw laser point cloud data for the entire survey in *.las (ASPRS v. 1.4) format. Convert data to orthometric elevations by applying a geoid correction.	RiProcess v1.8.5 TerraMatch v.19
Import raw laser points into manageable blocks to perform manual relative accuracy calibration and filter erroneous points. Classify ground points for individual flight lines.	TerraScan v.19
Using ground classified points per each flight line, test the relative accuracy. Perform automated line-to-line calibrations for system attitude parameters (pitch, roll, heading), mirror flex (scale) and GPS/IMU drift. Calculate calibrations on ground classified points from paired flight lines and apply results to all points in a flight line. Use every flight line for relative accuracy calibration.	TerraMatch v.19 RiProcess v1.8.5
Apply refraction correction to all subsurface returns.	LAS Monkey 2.4.0 (QSI proprietary software)
Classify resulting data to ground and other client designated ASPRS classifications (Table 6). Assess statistical absolute accuracy via direct comparisons of ground classified points to ground control survey data.	TerraScan v.19 TerraModeler v.19
Generate bare earth models as triangulated surfaces. Generate highest hit models as a surface expression of all classified points. Export all surface models in ERDAS Imagine (.img) format at a 3.0 foot pixel resolution.	TerraScan v.19 TerraModeler v.19 ArcMap v. 10.3.1
Correct intensity values for variability and export intensity images as GeoTIFFs at a 1.5 foot pixel resolution.	ArcMap v. 10.3.1 Las Product Creator 3.0 (QSI proprietary software)

Bathymetric Refraction

Green lidar pulses that enter the water column must have their position corrected for refraction of the light beam as it passes through the water and its resulting decreased speed. QSI has developed proprietary software (Las Monkey) to perform this processing based on Snell's law. The first step is to develop a water surface model (WSM) from the NIR lidar water surface returns. The water surface model used for refraction is generated using NIR points within the breaklines defining the water's edge. Points are filtered and edited to obtain the most accurate representation of the water surface and are used to create a water surface model TIN. A TIN model is preferable to a raster based water surface model to obtain the most accurate angle of incidence during refraction.

Once the WSM is generated, the Las Monkey refraction software then intersects the partially submerged green pulses with the WSM to determine the angle of incidence with the water surface and the submerged component of the pulse vector. This provides the information necessary to correct the position of underwater points by adjusting the submerged vector length and orientation. After refraction, the points are compared against bathymetric check points to assess accuracy.

Figure 5: A view of the Platte River topobathymetric digital elevation model colored by elevation, and overlaid with the above-ground lidar returns colored using RGB imagery.

Topobathymetric DEMs

Bathymetric bottom returns can be limited by depth, water clarity, and bottom surface reflectivity. Water clarity and turbidity affects the depth penetration capability of the green wavelength laser with returning laser energy diminishing by scattering throughout the water column. Additionally, the bottom surface must be reflective enough to return remaining laser energy back to the sensor at a detectable level. It is not unexpected to have no bathymetric bottom returns in turbid or non-reflective areas. As a result, creating digital elevation models (DEMs) presents a challenge with respect to interpolation of areas with no returns. Traditional DEMs are "unclipped", meaning areas lacking ground returns are interpolated from neighboring ground returns (or breaklines in the case of hydro-flattening), with the assumption that the interpolation is close to reality. In bathymetric modeling, these assumptions are prone to error because a lack of bathymetric returns can indicate a change in elevation that the laser can no longer map due to increased depths. The resulting void areas may suggest greater depths, rather than similar elevations from neighboring bathymetric bottom returns. Therefore, QSI created a water polygon with bathymetric coverage to delineate areas with successfully mapped bathymetry. This shapefile was used to control the extent of the delivered clipped topobathymetric model to avoid false triangulation (interpolation from TIN'ing) across areas in the water with no bathymetric returns.

Intensity Images

The difference in emitted wavelengths of the NIR (1064 nm) and Green (532 nm) lasers results in variation of the intensity information returned to the sensor for each laser. Additionally, the near-infrared wavelength is subject to spectral absorption by water, which can result in no returns over water surfaces. Due to these factors, QSI created one set of intensity images from NIR laser first returns, as well as one set of intensity images from green laser first returns.

Hydro-flattening and Water's Edge Breaklines

Hydro-flattening of closed water bodies was performed through a combination of automated and manual detection and adjustment techniques designed to identify water boundaries and water levels. Boundary polygons were developed using an algorithm which weights lidar-derived slopes, intensities, and return densities to detect the water's edge. The water edges were then manually reviewed and edited as necessary.

For the Platte River Fall 2019 project area all lakes and ponds outside of the area's main river channel were flattened to a consistent water level. The hydro-flattening process eliminates artifacts in the digital terrain model caused by both increased variability in ranges or dropouts in laser returns due to the low reflectivity of water. Once polygons were developed, the initial ground classified points falling within water polygons were reclassified as water points to omit them from the final ground model. Elevations were then obtained from the filtered lidar returns to create the final breaklines.

Water boundary breaklines were then incorporated into the hydro-flattened DEM by enforcing triangle edges (adjacent to the breakline) to the elevation values of the breakline. This implementation corrected interpolation along the hard edge. Water surfaces were obtained from a TIN of the 3-D water edge breaklines resulting in the final hydro-flattened model.

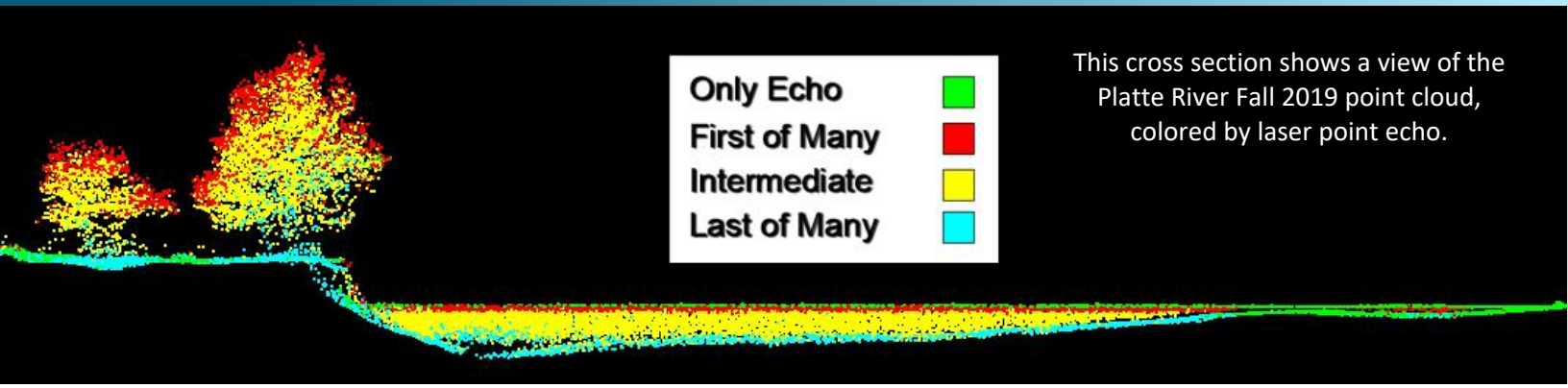

This cross section shows a view of the Platte River Fall 2019 point cloud, colored by laser point echo.

Bathymetric Data Coverage

To assist in evaluating performance results of the sensor throughout the life of the project, a polygon layer was created to delineate areas where bathymetry was successfully mapped for each year of data collection over the Platte River Fall project site. Insufficiently mapped areas were identified by triangulating bathymetric bottom points with an edge length maximum of 15.2 feet (4.56 meters). This ensured all areas of no returns > 100 ft^2 (> 9 m^2), were identified as data voids. The table below provides basic summary statistics about overall river size and bathymetric data coverage between 2016 and 2019. For the Fall 2019 survey, approximately 87% of the Platte River was successfully mapped with bathymetric bottom lidar returns.

Table 8: Bathymetric Coverage by Year

Data Collection Year	Total Water (acres)	Covered (acres)	Void (acres)	Covered (%)	Void (%)
2016	7,668.15	6,182.83	1,485.32	80.63%	19.37%
2017	7,465.07	5,816.21	1,648.86	77.91%	22.09%
2018	6,940.51	5,292.1	1,648.41	76.25%	23.75%
2019	12,610.03	10,996.2	1,613.83	87.20%	12.80%

First Return Lidar Point Density

The acquisition parameters were designed to acquire an average first-return density of 6 points/m^2. First return density describes the density of pulses emitted from the laser that return at least one echo to the system. Multiple returns from a single pulse were not considered in first return density analysis. Some types of surfaces (e.g., breaks in terrain, water and steep slopes) may have returned fewer pulses than originally emitted by the laser.

First returns typically reflect off the highest feature on the landscape within the footprint of the pulse. In forested or urban areas the highest feature could be a tree, building or power line, while in areas of unobstructed ground, the first return will be the only echo and represents the bare earth surface.

The average first-return density of the Platte River Fall 2019 lidar project was 2.58 points/ft^2 (27.80 points/m^2) (Table 9). The statistical and spatial distributions of all first return densities per 100 m x 100 m cell are portrayed in Figure 6 and Figure 8.

Bathymetric and Ground Classified Lidar Point Densities

The density of ground classified LiDAR returns and bathymetric bottom returns were also analyzed for this project. Terrain character, land cover, and ground surface reflectivity all influenced the density of ground surface returns. In vegetated areas, fewer pulses may have penetrated the canopy, resulting in lower ground density. Similarly, the density of bathymetric bottom returns was influenced by turbidity, depth, and bottom surface reflectivity. In turbid areas, fewer pulses may have penetrated the water surface, resulting in lower bathymetric density.

The ground and bathymetric bottom classified density of lidar data for the Platte River Fall 2019 project was 1.14 points/ft^2 (12.24 points/m^2) (Table 9). The statistical and spatial distributions ground classified and bathymetric bottom return densities per 100 m x 100 m cell are portrayed in Figure 7 and Figure 8.

Additionally, for the Platte River Fall 2019 project, density values of only bathymetric bottom returns were calculated for areas containing at least one bathymetric bottom return. Areas lacking bathymetric returns (voids)were not considered in calculating an average density value. Within the successfully mapped area, a bathymetric bottom return density of 0.90 points/ft^2 (9.70 points/m^2) was achieved.

Table 9: Average Lidar point densities

Density Type	Point Density
First Returns	2.58 points/ft² 27.80 points/m²
Ground and Bathymetric Bottom Classified Returns	1.14 points/ft² 12.24 points/m²
Bathymetric Bottom Classified Returns	0.90 points/ft² 9.70 points/m²

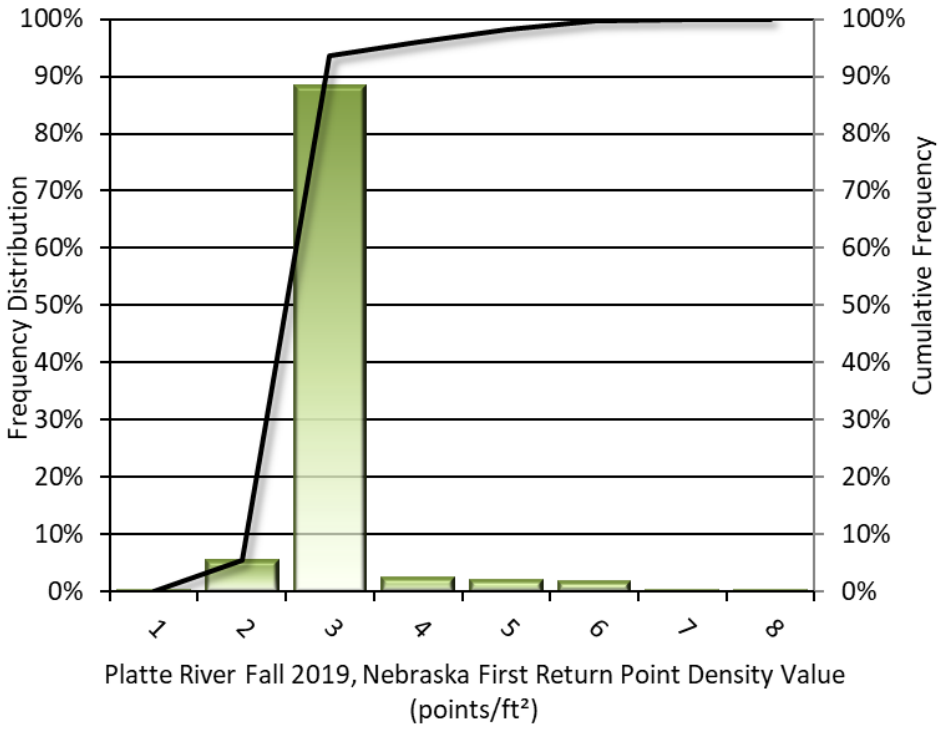

Figure 6: Frequency distribution of first return densities per 100 x 100 m cell

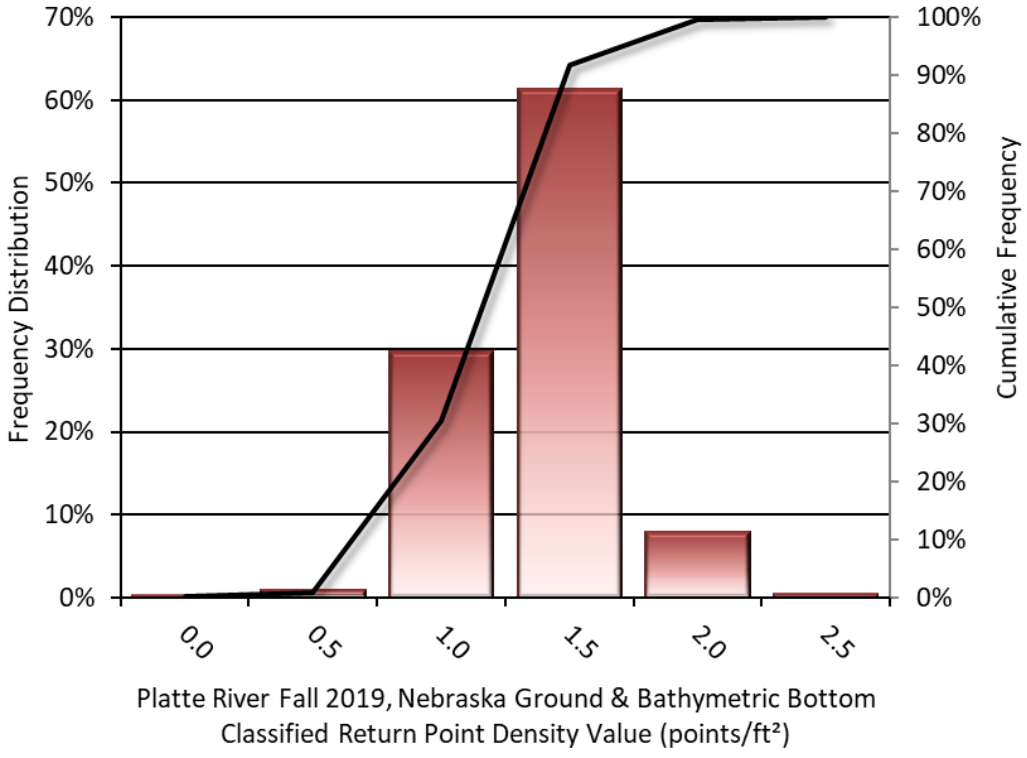

Figure 7: Frequency distribution of ground and bathymetric bottom classified return densities per 100 x 100 m cell

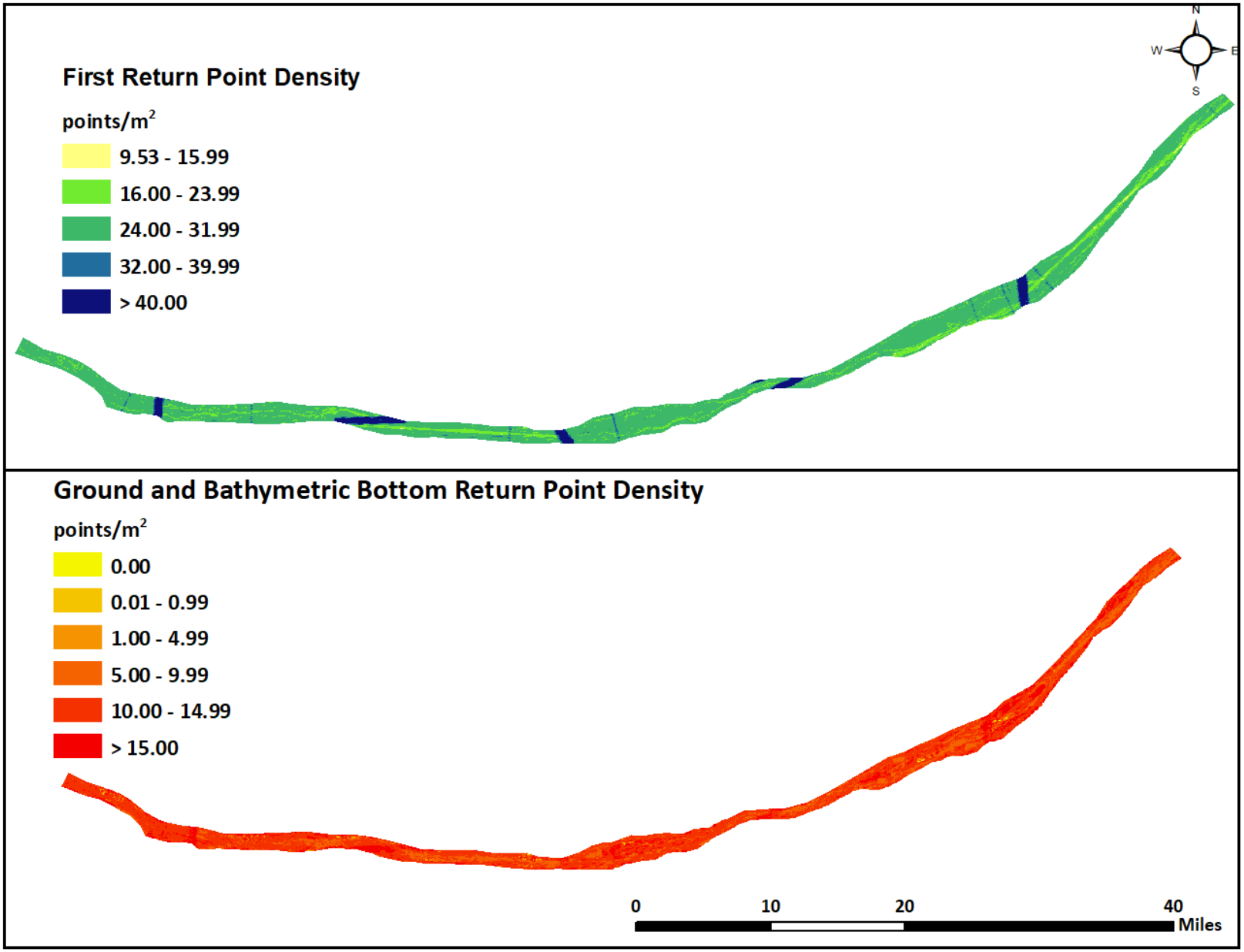

Figure 8: First return and ground and bathymetric bottom density map for the Platte River Fall 2019 site (100 m x 100 m cells)

Lidar Accuracy Assessments

The accuracy of the lidar data collection can be described in terms of absolute accuracy (the consistency of the data with external data sources) and relative accuracy (the consistency of the dataset with itself). See Appendix A for further information on sources of error and operational measures used to improve relative accuracy.

Lidar Non-Vegetated Vertical Accuracy

Absolute accuracy was assessed using Non-vegetated Vertical Accuracy (NVA) reporting designed to meet guidelines presented in the FGDC National Standard for Spatial Data Accuracy[1]. NVA compares known ground check point data that were withheld from the calibration and post-processing of the lidar point cloud to the triangulated surface generated by the unclassified lidar point cloud. NVA is a measure of the accuracy of lidar point data in open areas where the lidar system has a high probability of measuring the ground surface and is evaluated at the 95% confidence interval (1.96 * RMSE), as shown in Table 10.

The mean and standard deviation (sigma σ) of divergence of the ground surface model from ground check point coordinates are also considered during accuracy assessment. These statistics assume the error for x, y and z is normally distributed, and therefore the skew and kurtosis of distributions are also considered when evaluating error statistics. For the Platte River Fall 2019 survey, 20 ground check points were withheld from the calibration and post-processing of the lidar point cloud, with resulting non-vegetated vertical accuracy of 0.107 feet (0.033 meters), with 95% confidence (Figure 9).

QSI also assessed absolute accuracy using 888 ground control points. Although these points were used in the calibration and post-processing of the lidar point cloud, they still provide a good indication of the overall accuracy of the lidar dataset, and therefore have been provided in Table 10 and Figure 10.

Table 10: Absolute accuracy results

Absolute Vertical Accuracy		
	Non-Vegetated Check Points	**Ground Control Points**
Sample	20 points	888 points
95% Confidence (1.96*RMSE)	0.107 ft 0.033 m	0.115 ft 0.035 m
Average	0.006 ft 0.002 m	0.011 ft 0.003 m
Median	0.016 ft 0.005 m	0.010 ft 0.003 m
RMSE	0.055 ft 0.017 m	0.059 ft 0.018 m
Standard Deviation (1σ)	0.056 ft 0.017 m	0.058 ft 0.018 m

[1] Federal Geographic Data Committee, ASPRS POSITIONAL ACCURACY STANDARDS FOR DIGITAL GEOSPATIAL DATA EDITION 1, Version 1.0, NOVEMBER 2014. https://www.asprs.org/a/society/committees/standards/Positional_Accuracy_Standards.pdf.

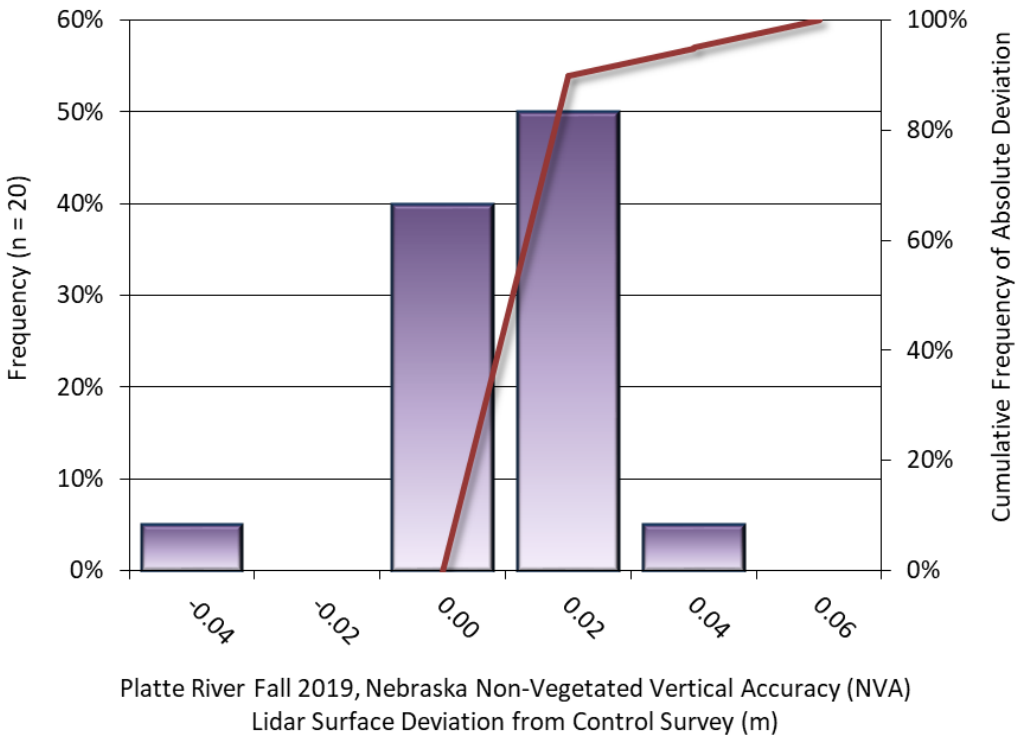

Figure 9: Frequency histogram for unclassified LAS deviation from ground check point values

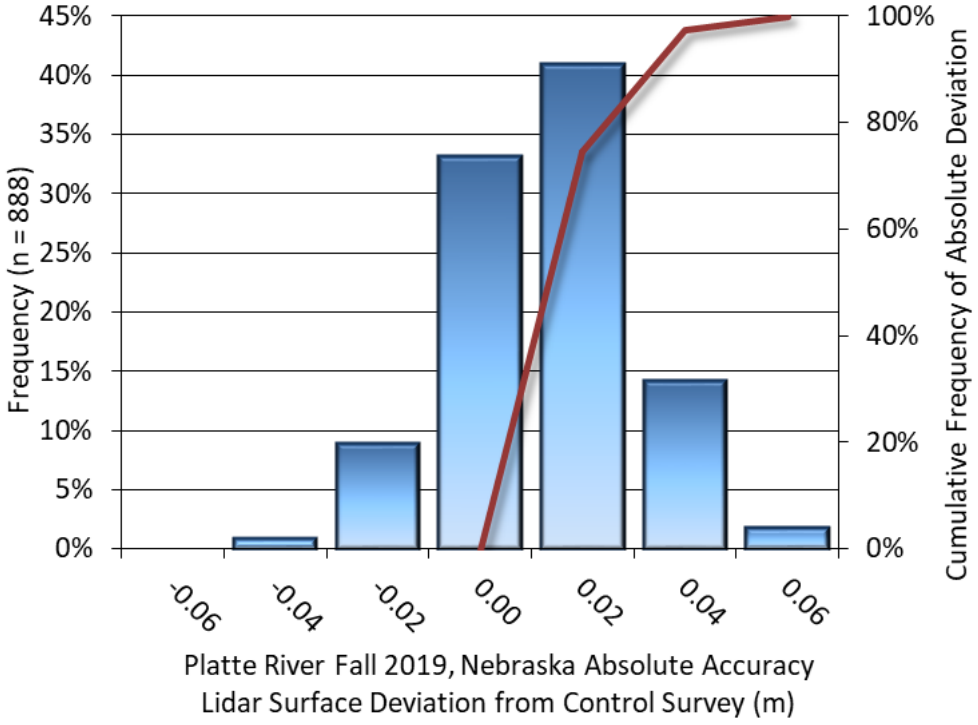

Figure 10: Frequency histogram for lidar surface deviation ground control point values

Lidar Bathymetric Vertical Accuracies

Bathymetric (submerged or along the water's edge) check points were also collected in order to assess the submerged surface vertical accuracy. Assessment of 128 submerged bathymetric check points resulted in a vertical accuracy of 0.749 feet (0.228 meters), while assessment of 51 wetted edge check points resulted in a vertical accuracy of 0.271 feet (0.083 meters), evaluated at 95% confidence interval (Table 11, Figure 11, Figure 12).

Table 11: Bathymetric Vertical Accuracy for the Platte River Fall 2019 Project

Bathymetric Vertical Accuracy (VVA)		
	Submerged Bathymetric Check Points	**Wetted Edge Bathymetric Check Points**
Sample	128 points	51 points
95% Confidence (1.96*RMSE)	0.749 ft 0.228 m	0.271 ft 0.083 m
Average Dz	-0.061 ft -0.018 m	-0.080 ft -0.024 m
Median	-0.115 ft -0.035 m	-0.072 ft -0.022 m
RMSE	0.382 ft 0.117 m	0.139 ft 0.042 m
Standard Deviation (1σ)	0.379 ft 0.115 m	0.114 ft 0.035 m

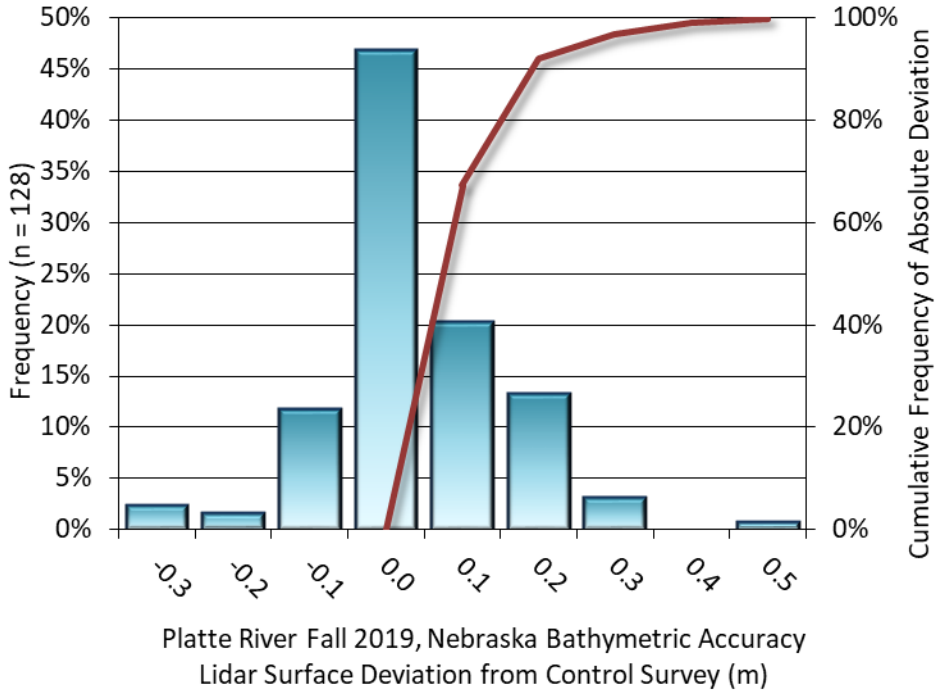

Figure 11: Frequency histogram for lidar surface deviation from submerged check point values

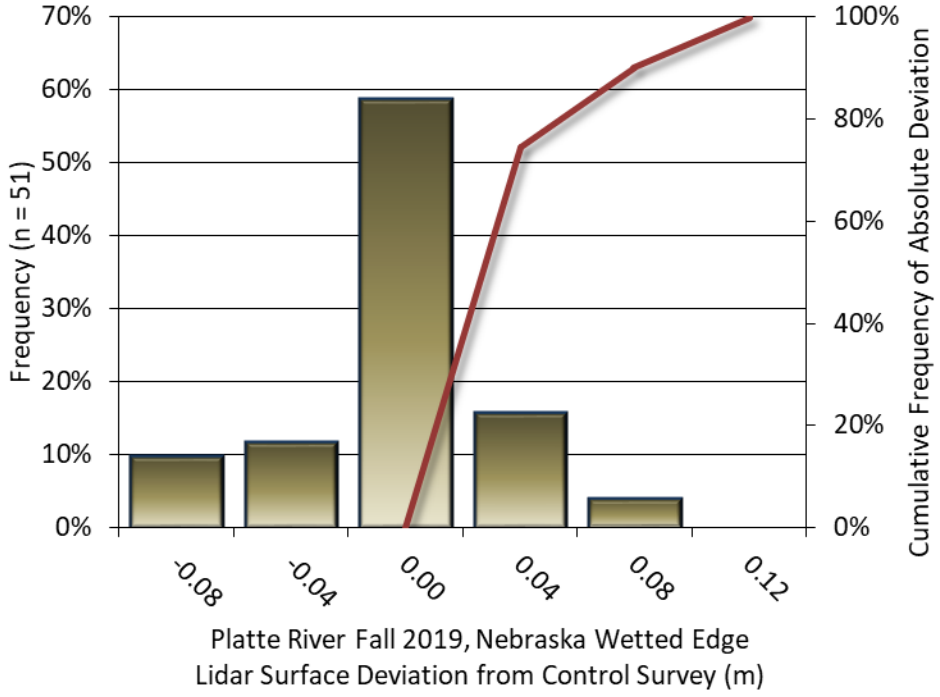

Figure 12: Frequency histogram for lidar surface deviation from wetted edge check point values

Lidar Relative Vertical Accuracy

Relative vertical accuracy refers to the internal consistency of the data set as a whole: the ability to place an object in the same location given multiple flight lines, GPS conditions, and aircraft attitudes. When the lidar system is well calibrated, the swath-to-swath vertical divergence is low (<0.10 meters). The relative vertical accuracy was computed by comparing the ground surface model of each individual flight line with its neighbors in overlapping regions. The average (mean) line to line relative vertical accuracy for the Platte River Fall 2019 Lidar project was 0.070 feet (0.021 meters) (Table 12, Figure 13).

Table 12: Relative accuracy results

Relative Accuracy	
Sample	349 flight line surfaces
Average	0.070 ft 0.021 m
Median	0.069 ft 0.021 m
RMSE	0.070 ft 0.021 m
Standard Deviation (1σ)	0.010 ft 0.003 m
1.96σ	0.020 ft 0.006 m

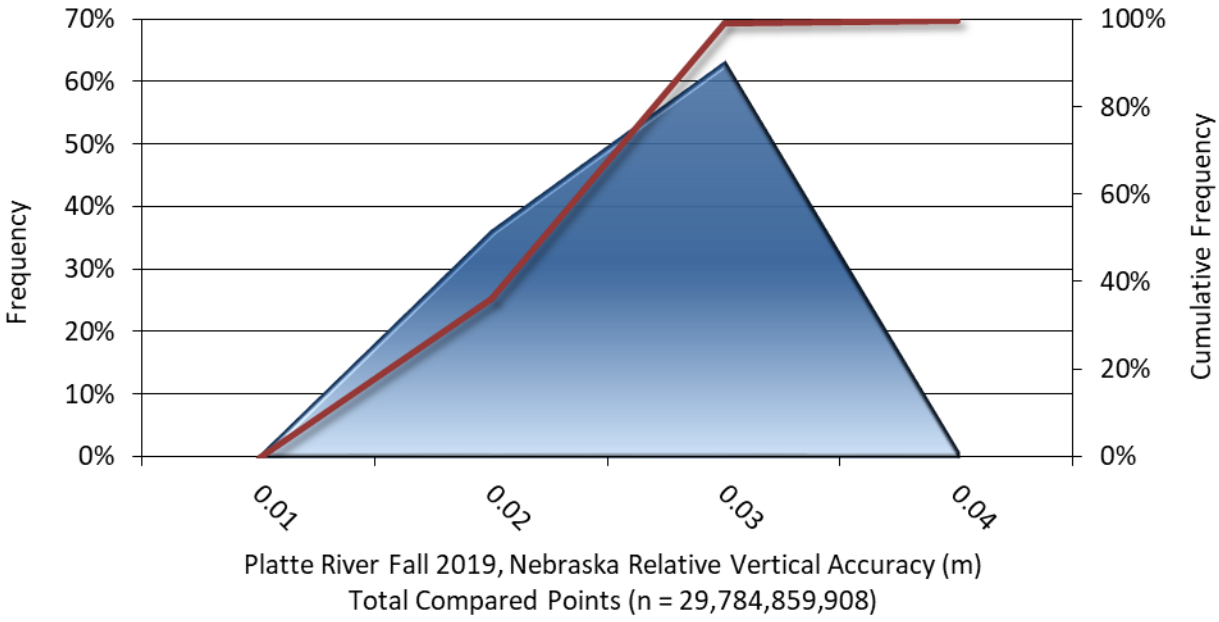

Figure 13: Frequency plot for relative vertical accuracy between flight lines

Lidar Horizontal Accuracy

Lidar horizontal accuracy is a function of Global Navigation Satellite System (GNSS) derived positional error, flying altitude, and INS derived attitude error. The obtained $RMSE_r$ value is multiplied by a conversion factor of 1.7308 to yield the horizontal component of the National Standards for Spatial Data Accuracy (NSSDA) reporting standard where a theoretical point will fall within the obtained radius 95 percent of the time. Based on a flying altitude of 450 meters, an IMU error of 0.002 decimal degrees, and a GNSS positional error of 0.015 meters, this project was compiled to meet 0.655 feet (0.200 m) horizontal accuracy at the 95% confidence level.

Table 13: Horizontal Accuracy

Horizontal Accuracy	
$RMSE_r$	0.10 ft 0.03 m
ACC_r	0.18 ft 0.06 m

GLOSSARY

1-sigma (σ) Absolute Deviation: Value for which the data are within one standard deviation (approximately 68th percentile) of a normally distributed data set.

1.96 * RMSE Absolute Deviation: Value for which the data are within two standard deviations (approximately 95th percentile) of a normally distributed data set, based on the FGDC standards for Non-vegetated Vertical Accuracy (FVA) reporting.

Accuracy: The statistical comparison between known (surveyed) points and laser points. Typically measured as the standard deviation (sigma σ) and root mean square error (RMSE).

> **Absolute Accuracy:** The vertical accuracy of Lidar data is described as the mean and standard deviation (sigma σ) of divergence of LiDAR point coordinates from ground survey point coordinates. To provide a sense of the model predictive power of the dataset, the root mean square error (RMSE) for vertical accuracy is also provided. These statistics assume the error distributions for x, y and z are normally distributed, and thus we also consider the skew and kurtosis of distributions when evaluating error statistics.
>
> **Relative Accuracy:** Relative accuracy refers to the internal consistency of the data set; i.e., the ability to place a laser point in the same location over multiple flight lines, GPS conditions and aircraft attitudes. Affected by system attitude offsets, scale and GPS/IMU drift, internal consistency is measured as the divergence between points from different flight lines within an overlapping area. Divergence is most apparent when flight lines are opposing. When the Lidar system is well calibrated, the line-to-line divergence is low (<10 cm).
>
> **Root Mean Square Error (RMSE):** A statistic used to approximate the difference between real-world points and the LiDAR points. It is calculated by squaring all the values, then taking the average of the squares and taking the square root of the average.

Data Density: A common measure of Lidar resolution, measured as points per square meter.

Digital Elevation Model (DEM): File or database made from surveyed points, containing elevation points over a contiguous area. Digital terrain models (DTM) and digital surface models (DSM) are types of DEMs. DTMs consist solely of the bare earth surface (ground points), while DSMs include information about all surfaces, including vegetation and man-made structures.

Intensity Values: The peak power ratio of the laser return to the emitted laser, calculated as a function of surface reflectivity.

Nadir: A single point or locus of points on the surface of the earth directly below a sensor as it progresses along its flight line.

Overlap: The area shared between flight lines, typically measured in percent. 100% overlap is essential to ensure complete coverage and reduce laser shadows.

Pulse Rate (PR): The rate at which laser pulses are emitted from the sensor; typically measured in thousands of pulses per second (kHz).

Pulse Returns: For every laser pulse emitted, the number of wave forms (i.e., echoes) reflected back to the sensor. Portions of the wave form that return first are the highest element in multi-tiered surfaces such as vegetation. Portions of the wave form that return last are the lowest element in multi-tiered surfaces.

Real-Time Kinematic (RTK) Survey: A type of surveying conducted with a GPS base station deployed over a known monument with a radio connection to a GPS rover. Both the base station and rover receive differential GPS data and the baseline correction is solved between the two. This type of ground survey is accurate to 1.5 cm or less.

Post-Processed Kinematic (PPK) Survey: GPS surveying is conducted with a GPS rover collecting concurrently with a GPS base station set up over a known monument. Differential corrections and precisions for the GNSS baselines are computed and applied after the fact during processing. This type of ground survey is accurate to 1.5 cm or less.

Scan Angle: The angle from nadir to the edge of the scan, measured in degrees. Laser point accuracy typically decreases as scan angles increase.

Native LiDAR Density: The number of pulses emitted by the Lidar system, commonly expressed as pulses per square meter.

Relative Accuracy Calibration Methodology:

Manual System Calibration: Calibration procedures for each mission require solving geometric relationships that relate measured swath-to-swath deviations to misalignments of system attitude parameters. Corrected scale, pitch, roll and heading offsets were calculated and applied to resolve misalignments. The raw divergence between lines was computed after the manual calibration was completed and reported for each survey area.

Automated Attitude Calibration: All data was tested and calibrated using TerraMatch automated sampling routines. Ground points were classified for each individual flight line and used for line-to-line testing. System misalignment offsets (pitch, roll and heading) and scale were solved for each individual mission and applied to respective mission datasets. The data from each mission were then blended when imported together to form the entire area of interest.

Automated Z Calibration: Ground points per line were used to calculate the vertical divergence between lines caused by vertical GPS drift. Automated Z calibration was the final step employed for relative accuracy calibration.

Lidar accuracy error sources and solutions:

Type of Error	Source	Post Processing Solution
GPS (Static/Kinematic)	Long Base Lines	None
	Poor Satellite Constellation	None
	Poor Antenna Visibility	Reduce Visibility Mask
Relative Accuracy	Poor System Calibration	Recalibrate IMU and sensor offsets/settings
	Inaccurate System	None
Laser Noise	Poor Laser Timing	None
	Poor Laser Reception	None
	Poor Laser Power	None
	Irregular Laser Shape	None

Operational measures taken to improve relative accuracy:

Low Flight Altitude: Terrain following was employed to maintain a constant above ground level (AGL). Laser horizontal errors are a function of flight altitude above ground (about 1/3000th AGL flight altitude).

Focus Laser Power at narrow beam footprint: A laser return must be received by the system above a power threshold to accurately record a measurement. The strength of the laser return (i.e., intensity) is a function of laser emission power, laser footprint, flight altitude and the reflectivity of the target. While surface reflectivity cannot be controlled, laser power can be increased and low flight altitudes can be maintained.

Reduced Scan Angle: Edge-of-scan data can become inaccurate. The scan angle was reduced to a maximum of ±20^{o} from nadir, creating a narrow swath width and greatly reducing laser shadows from trees and buildings.

Quality GPS: Flights took place during optimal GPS conditions (e.g., 6 or more satellites and PDOP [Position Dilution of Precision] less than 3.0). Before each flight, the PDOP was determined for the survey day. During all flight times, a dual frequency DGPS base station recording at 1 second epochs was utilized and a maximum baseline length between the aircraft and the control points was less than 13 nm at all times.

Ground Survey: Ground survey point accuracy (<1.5 cm RMSE) occurs during optimal PDOP ranges and targets a minimal baseline distance of 4 miles between GPS rover and base. Robust statistics are, in part, a function of sample size (n) and distribution. Ground survey points are distributed to the extent possible throughout multiple flight lines and across the survey area.

50% Side-Lap (100% Overlap): Overlapping areas are optimized for relative accuracy testing. Laser shadowing is minimized to help increase target acquisition from multiple scan angles. Ideally, with a 50% side-lap, the nadir portion of one flight line coincides with the swath edge portion of overlapping flight lines. A minimum of 50% side-lap with terrain-followed acquisition prevents data gaps.

Opposing Flight Lines: All overlapping flight lines have opposing directions. Pitch, roll and heading errors are amplified by a factor of two relative to the adjacent flight line(s), making misalignments easier to detect and resolve.